International Journal of Smart and Nano Materials, 2013
http://dx.doi.org/10.1080/19475411.2013.872207

Nano/microscale pyroelectric energy harvesting: challenges and opportunities

Devashish Lingam[a], Ankit R. Parikh[a], Jiacheng Huang[a], Ankur Jain[b] and Majid Minary-Jolandan[a]*

[a]*Department of Mechanical Engineering, NanoTech Institute, The University of Texas at Dallas, Richardson, TX 75080, USA;* [b]*Department of Mechanical and Aerospace Engineering, The University of Texas at Arlington, Arlington, USA*

(*Received 5 October; final version received 1 December 2013*)

With the ever-growing demand for renewable energy sources, energy harvesting from natural resources has gained much attention. Energy sources such as heat and mechanical motion could be easily harvested based on pyroelectric, thermoelectric, and piezoelectric effects. The energy harvested from otherwise wasted energy in the environment can be utilized in self-powered micro and nano devices, and wearable electronics, which required only μW–mW power. This article reviews pyroelectric energy harvesting with an emphasis on recent developments in pyroelectric energy harvesting and devices at micro/nanoscale. Recent developments are presented and future challenges and opportunities for more efficient materials and devices with higher energy conversion efficiency are also discussed.

Keywords: pyroelectricity; energy harvesting; micro/nanoscale; nanowires; composites; flexible devices; self-powered devices

1. Introduction

1.1. Demand for energy harvesting

Historically, batteries have always been the primary source of energy for powering low-power electronics, medical devices, and other embedded systems. Due to the perpetual need for increasing the efficiency and lifetime of these devices, energy harvesting from ambient sources like solar power, mechanical vibrations, and thermal energy, among others, have been considered [1,2]. Tapping into these renewable sources of energy offers solutions to the energy crisis and the ever-increasing demand for renewable energy resources. Energy harvesting is an attractive technique for a wide variety of self-powered micro devices or systems, for example, sensors, monitoring devices, biomedical devices, and implantable biodevices. In the last few years, the interest in energy harvesting has grown tremendously due to the exponential increase in the number of devices. The power requirements of these devices in large numbers put a considerable load on existing infrastructures and demands for much more efficient and novel sources of energy. The current usage of batteries in most personal devices has fueled research in improved battery technologies, but there is a critical need for self-powered, small-scale power generation

*Corresponding author. Email: majid.minary@utdallas.edu

devices that can supplement the existing technologies and eventually be able to replace batteries as the primary power source.

Energy harvesting can give rise to self-powered, maintenance-free devices with an almost inexhaustible source of energy [3]. Several devices from the millimeter scale down to the microscale have been manufactured, with an average power in the 10 μW–10 mW range [4,5]. Some examples of energy harvesting on the microscale include piezoelectric generators [3,6,7], thermoelectric microgenerators [8–10], photovoltaic devices (solar cells) [11,12], and electromagnetic microgenerators [13–15]. At small scale, pyroelectric materials are better suited for the conversion of thermal energy into electrical energy compared to thermoelectric devices, since they require temporal temperature gradient (dT/dt) instead of a spatial temperature gradient (dT/dx), which is more difficult to realize at micro/nanoscale [16]. Many pyroelectric materials are stable up to a very high temperature (~1200°C), which provides an advantage over thermoelectrics for harvesting energy form high-temperature sources. Furthermore, recent methods have been introduced to convert stationary spatial gradients to transient temperature gradients [17], which facilitates development of hybrid energy harvesters based on both thermoelectric and pyroelectric effects or radiation and pyroelectric effect [18]. In addition, devices based on pyroelectric energy harvesting require low or no maintenance since unlike piezoelectric energy harvesting devices, they do not include any moving parts. In recent years, alongside experimental implementation and developments, there have been several theoretical and numerical attempts for optimization of pyroelectric energy harvesting using mass, momentum, and energy equations [19–22]. These studies are critical for guiding future experimental efforts.

This paper provides a brief introduction to the pyroelectric effect and pyroelectric materials and summarizes recent developments in the harnessing of this effect for energy conversion. The origin of the pyroelectric effect, a detailed explanation on how the phenomenon occurs, and some of the factors affecting this effect have been discussed in Section 1.2. Common pyroelectric materials have been described along with their crystal class, crystal geometry, and Curie temperature in Section 2. Various existing methods for characterizing pyroelectric materials have been discussed briefly with illustrations in Section 3. Energy harvesting techniques and existing pyroelectric energy harvesters have been covered in Section 4. Section 5 provides concluding remarks on this review.

1.2. The pyroelectric effect

Pyroelectricity is one of the least-known electrical properties of solid materials. Theoretical treatment of pyroelectricity in terms of a change in net dipole moment has emerged in modern times, even though it has been known to mankind as a phenomenon for more than 24 centuries. This phenomenon was observed in the tourmaline crystal, which had the ability to attract straws and bits of wood [23]. In the two millennia that followed, scientists and writers were interested in the origin of the stone rather than physical explanations for the material attractive properties it displayed [24]. In 1717, the first scientific description of pyroelectricity was written in an article, but only in the nineteenth century did the quantitative understanding of this effect emerge [24].

Pyroelectricity is defined as the temperature-dependent spontaneous polarization in certain anisotropic crystals [24,25]. This effect refers to the generation of an electric

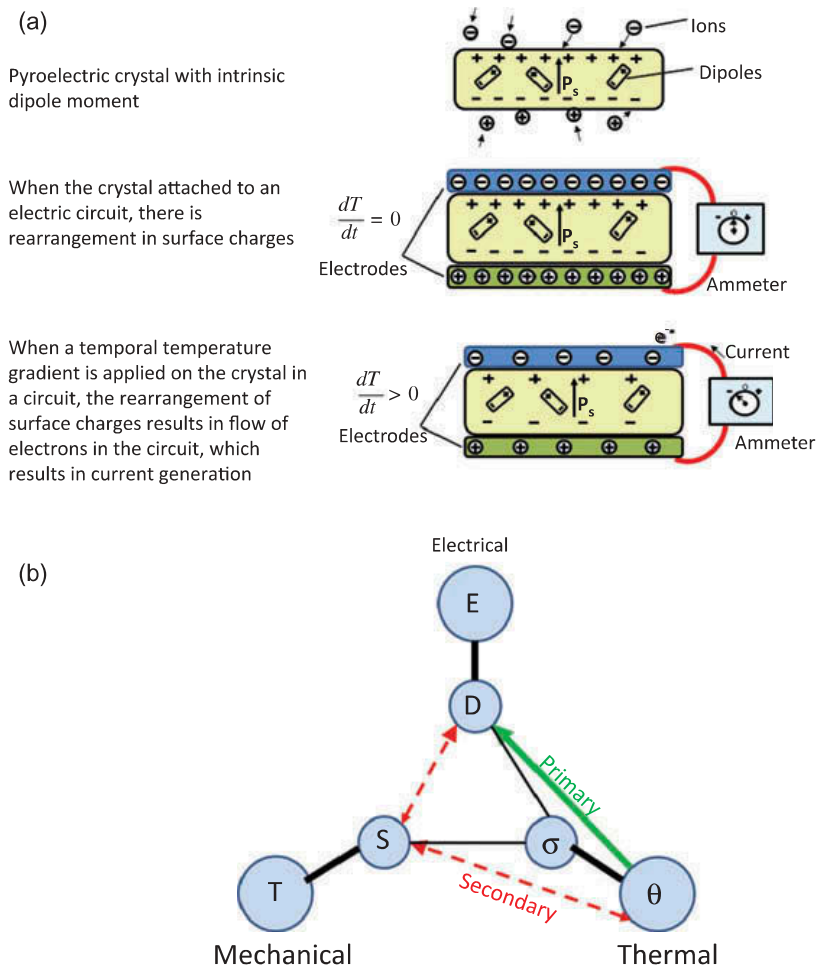

Figure 1. (a) Schematic shows the pyroelectric effect by changes in polarization under temperature change in a sample and the mechanism of electric charge harvesting from a pyroelectric material. (b) The diagram shows the definition of primary and secondary pyroelectric effects. Adapted with permission from Ref [24]. Copyright (2005), American Institute of Physics.

current/potential in materials with non-centrosymmetric crystal structure when subjected to a temporal temperature gradient (dT/dt) (Figure 1(a)). Pyroelectricity is exhibited by crystals belonging to the polar classes 1, 2m, 2mm, 3, 3m, 4, 4mm, 6, and 6mm [26,27]. Pyroelectric materials have a unique polar axis along which spontaneous polarization exits. The unit cell of pyroelectric materials has a dipole moment, and the dipole moment per unit volume of the material is called the spontaneous polarization [24]. A change in temperature causes the net dipole moment and hence the spontaneous polarization to change. The pyroelectric coefficient p is defined as the differential change in spontaneous polarization P caused by a change in temperature T [28]. In the most general form, for a stress-free material in an open circuit condition, the change in polarization due to change in temperature is expressed as follows:

$$\frac{\partial P_x}{\partial T} = \frac{\partial P_{x0}}{\partial T} + \frac{\partial (d_{xkl}\sigma_{kl})}{\partial T} \tag{1}$$

The first term on the right hand side of Equation (1) is the permanent polarization, and the second term represents the piezoelectric induced polarization [28]. Change in the polarization, causes change in surface bound charges, and hence redistribution of free charges in the material to compensate for the change in surface bound charges. In a test setup, this results in a pyroelectric current flow in the external circuit. If the circuit is open, the free charges simply remain in the electrodes and an electric potential is generated. The constraints in the definition of the pyroelectric coefficient are constant electric field E and constant elastic stress σ. Constant stress means that the crystal is not clamped, but completely free to expand or contract thermally. When the crystal is rigidly clamped under constant strain ε, to prevent expansion or contraction, a change in temperature causes a change in electric displacement signifying the primary pyroelectric effect (Figure 1(b)). The second contribution, the secondary pyroelectric effect, is a result of crystal deformation. Thermal expansion causes a strain that alters the electric displacement via a piezoelectric process. Direct measurement of the primary effect is rather difficult, but the secondary effect can be readily calculated from the values of the thermal expansion coefficient, the elastic stiffness, and the piezoelectric strain constant [24,26,27,29]. Therefore experimentally, the pyroelectric effect under the constraint of constant stress – the total effect – is what is usually measured. Moreover, it shows a distinction between ferroelectric and non-ferroelectric materials.

To understand this effect, let us consider a thin parallel-sided sample of material so cut that its crystallographic symmetry axis is perpendicular to the flat surfaces. The dipoles in a unit cell of a pyroelectric material are packed so that the components of the dipole moment in each unit cell add up in the direction normal to the flat surfaces. The dipole moment per unit volume exists in the absence of an applied electric field and is equivalent to a layer of bound charges on each flat surface of the sample. Nearby free charges such as electrons or ions will be attracted to the sample. We consider that the conductive electrodes are then attached to the surfaces and connected through an ammeter having a low internal resistance. If the temperature of the sample is constant, then the spontaneous polarization also remains constant and no current flows through the circuit. But in most pyroelectric materials, an increase in temperature causes the net dipole moment and consequently, the spontaneous polarization to decrease. The quantity of bound charge then decreases and the redistribution of free charges to compensate for the change in bound charge results in a current flow. If the sample is cooled instead of being heated, the current sign is reversed. The pyroelectric current is observed only during the period in which the temperature changes, i.e., when there exists temporal temperature gradient [30,31].

2. Most common pyroelectric materials

Pyroelectric materials currently find widespread use in thermal detectors and sensors, where the choice of the pyroelectric material is mainly determined by figure of merit, detector size, availability, durability, environment in which the material has to operate, thermal radiation levels to be detected, purpose for which the detector is employed, maximum ambient temperature of operation, and the range over which stable operation is required [32]. A wide selection of pyroelectric materials is necessary not only to improve the sensor performance but also to cater to specific sensor applications. In the following discussion, materials most commonly used in the industry are discussed with

respect to their Curie temperature. Curie temperature is the critical point where a non-polar material undergoes a structural transformation; below this critical point, the material exhibits an intrinsic, permanent electrical polarization, usually along a certain crystallographic axis [33]. Table 1 presents matrices for the 10 pyroelectric crystal classes and two pyroelectric Curie groups. Table 2 presents a summary of pyroelectric coefficient of various materials at room temperature.

(1) *Triglycine sulfate* (*TGS*) – $(NH_2CH_2COOH)_3H_2S0_4$: TGS constitutes a large family of isomorphous compounds. The compounds based upon TGS have provided some of the highest pyroelectric figures of merit ($5.5 \times 10^{-4}\,Cm^{-2}K^{-2}$) [23]. TGS possesses a Curie temperature of 49°C [34]; above this temperature, it exists as centrosymmetric class 2m, and below this temperature, it is a polar point group 2 with the polar axis along the monoclinic *b* axis. Since the glycine groups are polar in nature, the reversal is largely associated with the rotation of the glycine group about the crystallographic *a*-axis [23]. TGS pyroelectric crystals are primarily used in single element detectors where sensitivity of detection of temperature change is of prime importance.

(2) *Polyvinylidene fluoride (PVDF)*: PVDF is a ferroelectric polymer, which exhibits a strong piezoelectric effect. PVDF molecules have a repeat unit of $–CH_2–CF_2–$, which take up a number of stable configurations based on the polymers treatment. The polar unit configuration of the material crystal exhibits pyroelectric effect. PVDF has a Curie temperature up to 180°C, but the polar properties degrade when it is heated above 80°C. It finds applications in large area detectors for laser pulse monitoring and also single element devices such as intruder alarms. Large PVDF thin films are available commercially at low cost for use in detectors [23,32,35,36].

Table 1. Matrices for the 10 pyroelectric crystal classes and two pyroelectric Curie groups [33].

Point group	Pyroelectric metrics
1	$(p_1 \quad p_2 \quad p_3)^T$
2	$(0 \quad p_2 \quad 0)^T$
m	$(p_1 \quad 0 \quad p_3)^T$
*mm*2, 3, 3*m*, 4, 4*mm*, 6, 6*mm*, ∞, ∞*m*	$(0 \quad 0 \quad p_3)^T$

Table 2. Pyroelectric coefficient of various materials at room temperature, units $\mu C/m^2\,K$ [24,33].

Material	Experimental value	Secondary coefficient	Primary coefficient
Triglycine sulfate TGS (2)	–270	–330	60
$LiNbO_3$ (3m)	–83	+12.8	–95.8
$LiTaO_3$ (3m)	–176	–1	–175
$Pb_5Ge_3O_{11}$(3)	–95	+15.5	–110.5
$BaTiO_3$ (∞m)	–200	+60	–260
$PbZr_{0.95}Ti_{0.05}O_3$ (∞m)	–268	+37.7	–305.7
ZnO (6mm)	–9.4	–2.5	–6.9
CdSe (6mm)	–3.5	–0.56	–2.94
CdS (6mm)	–4.0	–1.0	–3.0

(3) *Lithium tantalate* (*$LiTaO_3$*): $LiTaO_3$ is an oxygen octahedral crystal consisting of layers of oxygen ions arranged in hexagonal close packing. It is used in single crystal form grown using the Czochralski method and exhibits a moderate pyroelectric effect. $LiTaO_3$ possesses a Curie temperature of 665°C. $LiTaO_3$ finds applications in pyroelectric detectors, and widespread usage in one-dimensional (*1D*) commercial detector arrays. $LiTaO_3$ has drawbacks such as high thermal diffusivity, which reduces its minimum resolvable temperature difference at high spatial frequencies. One of the solution used to resolve this problem is the use of ion beam reticulation to separate detector elements [23,32,35,37].

(4) *Gallium nitride* (*GaN*): GaN is a wurtzite-structured crystal. It is a natural pyroelectric with polarization in the *c*-axis. GaN exhibits a strong pyroelectric effect at temperature above 300°C, whereas $LiTaO_3$ and $PbTiO_3$ exhibit the property below 300°C, and hence, GaN finds applications in high-temperature environments [25,38–40]. The pyroelectric coefficient of thin GaN films were reported to be ~10^4 V/mK [38].

(5) *Zinc Oxide* (*ZnO*): ZnO is also a wurtzite-structured natural pyroelectric crystal with polarization in the *c*-axis. Most applications utilizing ZnO as the primary material use it in the thin film form. ZnO thin film has exhibited a conversion of thermal radiation 10 times larger than GaN films. ZnO possesses a Curie temperature of 430°C and a pyroelectric coefficient of 4×10^4 V/mK was observed from experiments conducted on a bundled arrays of nanowires [41–43].

(6) *Perovskite based pyroelectrics*: Perovskite is a large family of oxygen octahedral crystals with the general formula ABO_3 [23]. The perovskite structure undergoes deformation to give rhombohedral, tetragonal, or orthorhombic structures. In Lead Zirconate- and Lead Titanate-based structures, dopants are used to improve the pyroelectric properties of these ceramic-based pyroelectrics. Lead Titanate ($PbTiO_3$) possesses a high Curie temperature of 490°C and a high polarization rate. The preferred method of manufacturing devices is by deposition of thin film layers rather than machining from bulk.

3. Characterization of pyroelectric materials

Characterization of pyroelectric effect at the bulk level is rather straight forward. Often, two electrodes are connected to the polar axis of the material and the material is placed in an oven or on a hot plate or heated by a laser [33,44]. The temperature increase or decrease in the sample results in generation of electric current/voltage. Since the material is at bulk scale, the generated current/voltage is large enough that could be easily measured using conventional electronics. These methods are not applicable to small scales, such as to thin films and *1D* nanostructures since the proper electric contact to these materials is complicated. In addition, the generated current/voltage is small and demands high-sensitivity electronics to avoid any artifacts in the measurement. There are several methods for characterization of pyroelectric effect. Each method has advantages and disadvantages [44]. Below, we have provided a brief summary of the most common methods.

3.1. Continuous oscillation method (the 2ω method)

In this method, the sample is subjected to a continuous, sinusoidally modulated heat source (Figure 2(a)). The generated current or voltage is recorded with a lock-in amplifier

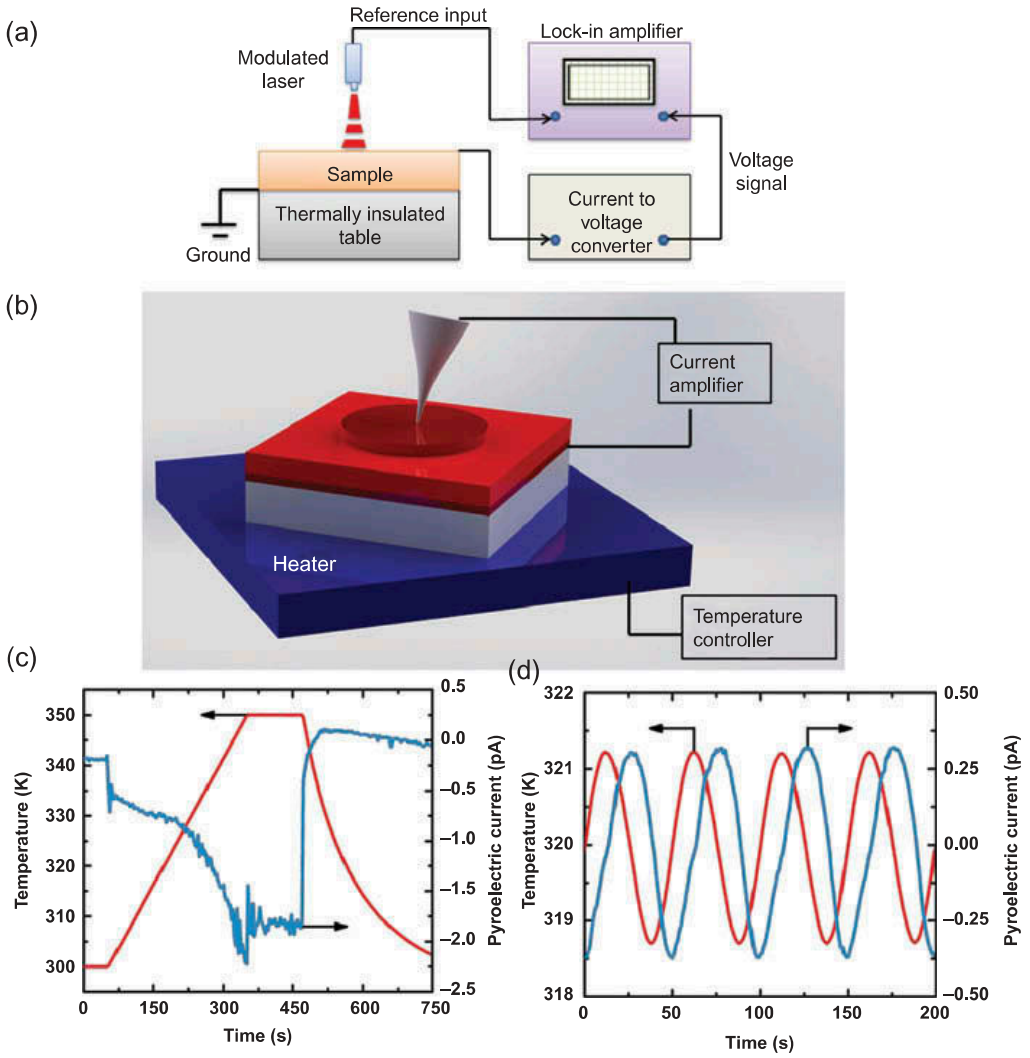

Figure 2. (a) Layout and equivalent circuit for the continuous oscillation (2ω) method. Reproduced with permission from Ref [30]. Copyright (2012), AIP Publishing LLC. (b) Layout for the direct and low frequency periodic measurement. (c) Pyroelectric current generated (blue) for the direct measurement [46]. (d) Pyroelectric current generated (blue) for the low-frequency periodic measurement [46]. Reproduced with permission from Ref [46]. Copyright (2012), AIP Publishing LLC.

[44]. When the modulation frequency is low enough and the capacitance-based impedance is negligible, it can be shown theoretically that the generated current from pyroelectricity is 90° out of phase with the thermal wave [44]. The current is measured using pre-amplifier circuits and is observed using oscilloscopes. When the heating rate from the thermal heat source is significantly smaller than the thermal diffusion in the sample, then the sample is heated uniformly rather than a sinusoidal modulation [44].

3.2. *Direct and low-frequency periodic measurement*

In the direct method, a poled sample is subjected to a linear temperature ramp with its electrodes shorted, which results in the generation of a pyroelectric current

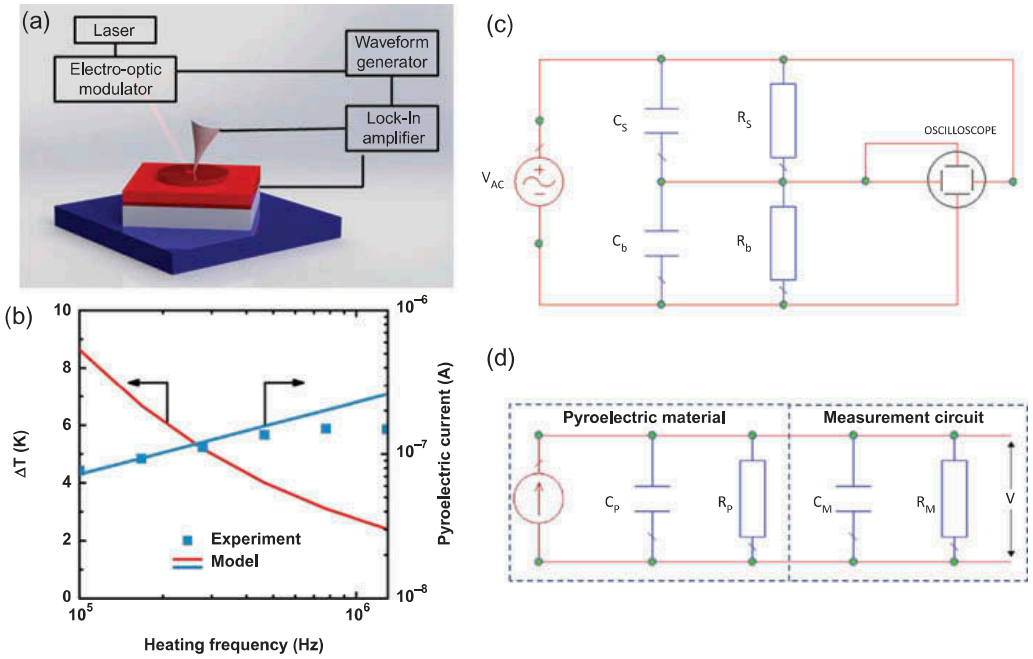

Figure 3. (a) Setup for the Laser Intensity Modulation Measurement (LIMM) method [46]. (b) A graph showing temperature oscillation amplitude and the pyroelectric current as a function of the heating (modulation) frequency. Reproduced with permission from Ref [46]. Copyright (2012), AIP Publishing LLC. (c) The Sawyer–Tower bridge, used for the constant temperature measurement method [30]. (d) Setup and equivalent circuit for the continuous temperature ramping method. Reproduced with permission from Ref [30]. Copyright (2012), AIP Publishing LLC.

(Figure 2(b–d)) [45–47]. In this method, the pyroelectric coefficient across the corresponding temperature range can be obtained [46]. However, the simultaneous existence of non-pyroelectric currents makes this technique difficult for use with thin films. The low-frequency periodic measurement technique utilizes a low-frequency sinusoidal temperature oscillation, which leads to a phase shift in the pyroelectric current [46]. The measured current is then fitted to a sine function to extract its phase and magnitude. The pyroelectric coefficient can then be obtained from the out of phase component of the pyroelectric current [46].

3.3. *Laser intensity modulation measurement (LIMM)*

This method uses an intensity-modulated laser beam to generate periodic temperature oscillations on the surface of the thin film (Figure 3(a)) [46]. The surfaces of the sample are coated with opaque electrodes using a sputtering or evaporation process [48]. The sample is then mounted in a vacuum chamber with optical windows through which the sample can be irradiated [48]. The laser is modulated over a wide frequency range (Hz–kHz, kHz–MHz) using an acousto-optic modulator, and the pyroelectric current generated at a specific modulation frequency is measured using a lock-in amplifier [46,48]. The pyroelectric effect is observed closer to the top surface of the thin film due to an increasing modulation frequency [46,49]. A variation of this method is the Surface Laser Intensity Modulation Measurement (SLIMM), where the data are obtained from a

single surface and the modulation frequencies used are much higher compared to LIMM [50]. LIMM is much more suited for determining the polarization distribution near the free surface of the sample [50].

3.4. Constant temperature measurement

This measurement is valid only for pyroelectric materials with switchable polarization (ferroelectrics) [30]. This method uses a Sawyer–Tower bridge to obtain ferroelectric hysteresis loops through the magnitude of polarization induced in the sample (Figure 3(c)) [30]. A typical Sawyer–Tower bridge consists of a linear capacitor (a capacitor with linear response characteristics), with a capacitance (C_b) greater than that of the ferroelectric material. The resistor R_b in the circuit partly compensates for the ohmic conductivity present in most ferroelectric materials. The voltage measured across the linear capacitor is proportional to the charge stored on the surface of the ferroelectric material, which represents the polarization of the material in the absence of an electric current [30]. Accurate measurements require the hysteresis loop to be rectangular, which has only been observed in triglycine sulfate [30,51]. However, this technique has a drawback. The presence of displacement, ohmic, and charge-injection currents reduces the accuracy of the measurements and also affects the electric field in the sample, hence requiring circuitry which can detect the ohmic and charge injection currents [30].

3.5. Continuous temperature ramping

This method involves measuring the pyroelectric current flowing between two contacts on a sample, which is continuously heated or cooled, (Figure 3(d)) [30]. A uniform temperature distribution is obtained in the sample, when the sample heating rate is smaller than the time required for thermal diffusion [30]. The pyroelectric coefficient is then measured by one of two methods: the Lang–Steckel method [52] and the short circuit method used by Glass [53]. In the Lang–Steckel method, the pyroelectric material is connected to a high input impedance electrometer shunted by a calibrated resistor. The voltage measured by the electrometer is then used with the following expression to determine the pyroelectric coefficient of the sample [52]:

$$\frac{pA}{C_T} \times \frac{dT}{dt} = \frac{dV}{dt} + \frac{1}{R_T C_T} \times V \tag{2}$$

where C_T is the total capacitance of the pyroelectric element and the electrometer, p is the pyroelectric coefficient, A is the electrode area of the pyroelectric element, dT/dt is the instantaneous time derivative of the temperature, V and dV/dt are the electrometer voltage and the time derivative of voltage, respectively, and R_T is the total equivalent resistance of the pyroelectric element and the shunt resistor.

In the method used by Glass, the sample is heated under short circuit conditions to ensure a constant electric field across the sample [53]. This is done because dP/dT (rate of change of total polarization of the sample with temperature at constant stress) is also a function of the constant electric field [53]. The sample is connected to an operational amplifier and a feedback capacitor. The charge developed on the faces of the sample is integrated continuously using a ballistic galvanometer. The output voltage of the amplifier is plotted against the sample temperature, and the temperature derivative of this curve

gives the pyroelectric coefficient [53]. Compared to the Lang–Steckel method, the short circuit method does not require the rate of change of temperature to measure the change in polarization of the sample, but it gives an average value of the pyroelectric coefficient and not an absolute value [30].

4. Energy harvesting

As smart materials, pyroelectric materials have found applications in an array of fields. The most prominent fields are energy harvesting and applications in sensors. For energy harvesting, they convert the thermal energy to electricity, and in sensors, they are used as sensing elements to detect heat (or indirectly motion) signals by conversion into an electric signal. We limit this section to energy harvesting application, in particular recent progress on nanowire, nanofibers, and thin film pyroelectrics.

The detectable current $i_p(t)$ of a pyroelectric material is proportional to the rate of change of its temperature [54], and can be expressed as follows:

$$i_p(t) = pA\frac{dT(t)}{dt} \tag{3}$$

In this equation, p is the pyroelectric coefficient of the material, which is measured experimentally by measuring the output current. It is evident that the pyroelectric coefficient is one of the most important factors influencing the performance of a pyroelectric material: the higher the pyroelectric coefficient, the better the pyroelectric performance. The values for p for various materials are given in Table 2. In Equation (3), A is the surface area of the electrode connected to the pyroelectric material during measurements. Larger electrode will collect larger number of electrons and hence the measured current will increase. dT/dt denotes the temporal temperature gradient. Larger changes in temperature in shorter periods of time generate larger output current. Hence large temperature gradients such as in engine of automobiles or in turbines are attractive for this purpose [55].

In terms of modeling, the pyroelectric generator is modeled as a current source with a capacitor and a resistor in parallel. The current is generated within the pyroelectric element with the change in temperature. However, one of the main problems of pyroelectric energy harvesting is a heating process followed by a cooling process, which produces charge accumulation in different directions. One way to mitigate this problem is to use a full bridge diode rectifier circuit. It has been also demonstrated that stationary spatial temperature gradients can be converted into required transient temperature for pyroelectric energy harvesting [56]. One of the proposed methods includes a micro heat engine that acts as a thermal energy shuttle between a heat sink and a heat source. In this configuration, an oscillating thermal field is created across a pyroelectric generator (Figure 4) [17]. It was demonstrated that using this micro thermomechanic–pyroelectric energy generator (μTMPG), 3 μW power could be harvested for a temperature difference of 79.5 K from pyroelectric generators.

Using similar methods, hybrid energy harvesting devices could be developed that operate for both thermoelectric and pyroelectric energy harvesting [57]. Laminating materials in composite form have been also discussed as methods of enhancing pyroelectric energy harvesting by changing the effective thermal mass of the system [58].

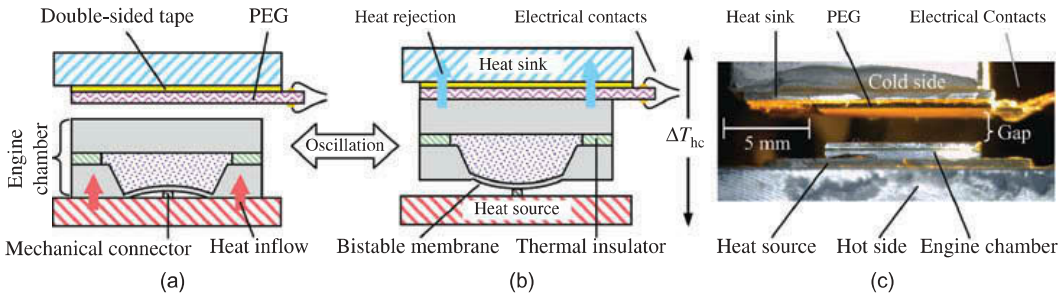

Figure 4. Illustration of the μTMPG technique for converting stationary spatial temperature gradient into transient temperature gradient. Reproduced with permission from Ref [17]. Copyright (2011), AIP Publishing LLC.

Pyroelectric energy harvesting has been demonstrated in thin films, nanowires, and nanofibers. In particular, thin films offer a large surface area for enhanced thermal exchange and larger electrodes, and hence larger current output [59–61]. Recent advances in nanotechnology have enabled energy harvesting from 1D materials such as nanowires and nanofibers (Figure 5) [43]. Theoretical studies have predicted pyroelectric size-effect enhancement for nanowires, and hence, they hold great promise for nanoscale pyroelectric energy harvesting [31]. The advantages of nanowires are that they have enhanced mechanical properties compared to the bulk materials [62]. The enhanced mechanical properties are often because of lower defect density in these materials. As such, nanowires can withstand larger strains to failure. This attribute makes them attractive for flexible nanogenerators, which are promising for wearable electronics (Figure 5(d)) [63,64].

In addition, nanowires have already demonstrated to show enhanced piezoelectric and thermoelectric properties compared to their bulk counterparts [65–69]. These enhancements are often due to lower defect density in the nanowire form compared to the bulk form, which may also contribute to the pyroelectric enhancement. For example, for ZnO nanowires, pyroelectric current and voltage coefficients of ~1.2–1.5 nC/cm^{2}K and ~2.5–4.0 × 10^4 V/mK have been estimated from experimental studies on an array of bundled nanowires [43]. These values are larger than the values for the bulk and thin films (~1 nC/cm^{2}K).

Recently, it was shown that single pyroelectric microwire of PZT can be used to power temperature sensors [70]. In this experiment, single lead zirconium titanate (PZT) microwire was placed on a glass substrate and was fixed with silver paste as electrodes at its two ends. The entire device was then packaged into polydimethylsiloxane (PDMS). After electric poling at a voltage of 3.5 kV, the device was placed on a heater to generate temporal temperature changes for pyroelectric energy harvesting. It was shown that the response time of the sensor was 0.9 second and the minimum detectable temperature was 0.4 K at room temperature.

Nanowires are also incorporated into composite structures enabling development of high-performance materials. Nanogenerators based on cost-effective and easily accessible materials such as $KNbO_3$ were recently demonstrated [63]. Hybrid and flexible thermal–mechanical–solar energy harvesting devices have been also introduced, with PVDF thin film as the pyroelectric element [71]. It was demonstrated that the nanogenerator can drive a LCD using the hand touching, which has both mechanical and thermal components. The PVDF thin film can be fabricated using spin coating process to desired thickness.

In addition to nanowires, nanofibers are also attractive for pyroelectric energy harvesting. Nanofibers are often mechanically soft and can be readily incorporated into flexible

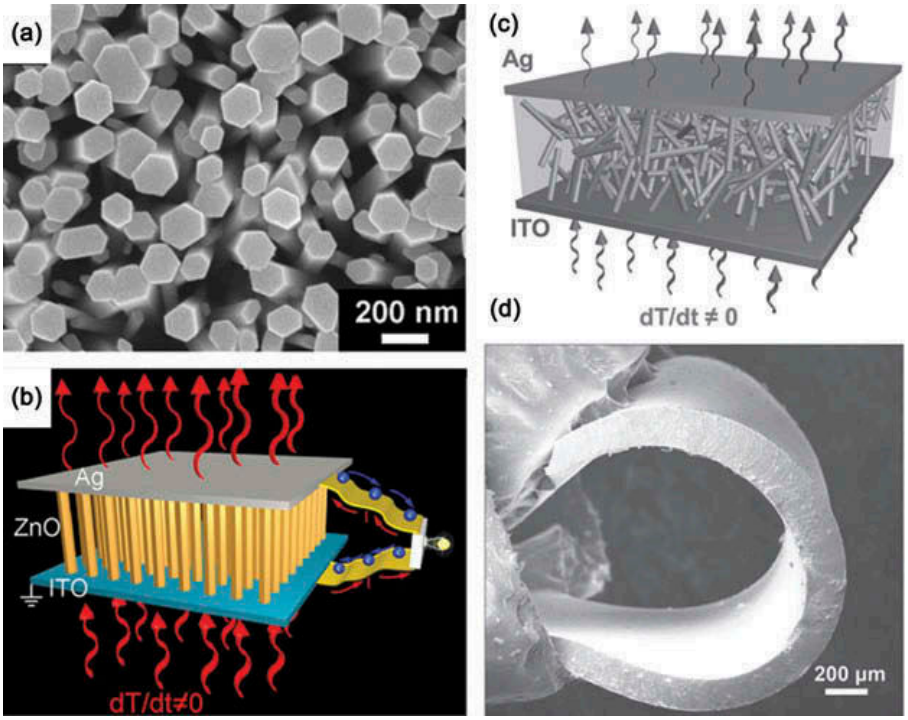

Figure 5. Pyroelectric energy harvesting from nanowires and nanowire composites. (a), (b) vertical bundle of ZnO nanowires are sandwiched between two electrodes. Reprinted with permission from Ref [43]. Copyright (2012) American Chemical Society. (c), (d) flexible pyroelectric nanogenerator based on $KNbO_3$ nanowire composites. Reprinted with permission from Ref [63]. Copyright (2012) John Wiley and Sons.

devises [72–74]. Nanofibers are mostly fabricated using electrospinning technique [75]. In this technique, a high DC voltage between the liquid in a syringe and a collector spins nanofibers in diameters from several tens of nanometers to several microns. The most notable pyroelectric material that is produced using this method is PVDF and its co-polymer poly (vinylidene fluoride-trifluoroethylene) (PVDF-TrFE) [76,77]. Recent developments of PVDF for use in microgenerators for portable devices make it an area of interest for self-powering devices [78]. PVDF is a high-performance engineering thermoplastic which shows excellent mechanical and physical behavior. It is also chemically inert toward most acids, organics, aliphatic and aromatic compounds, solvents, oxidants, halogens, and alcohol [79]. Although PVDF pyroelectric harvesters gain limited energy and voltage, these devices will gain a considerable voltage and energy with a larger element area. In PVDF, the beta (β) phase contributes to the piezoelectric and pyroelectric effects, hence the PVDF fibers need to be poled or mechanically stretched to increase the relative content of β phase [80,81]. Hence, for higher efficiency energy harvesting higher content of β phase is desirable.

Energy harvesting of waste heat from pyroelectric materials can be achieved by utilizing the Olsen cycle [82–85]. The Olsen cycle consists of two isothermal and two isoelectric field processes in the electric displacement–electric field (D–E) diagram. The principle of the Olsen cycle is to charge a capacitor via cooling under low electric field and to discharge it under heating at a higher electric field. Possibility of capturing thermal energy derived from natural heating of pavements, storing the energy, and using it as an

alternative power source for other devices has been also recently explored. In this study, pyroelectric materials were used as the energy harvester. Single and polycrystalline based materials and a polycrystalline composite material based on ordinary Portland cement with carbon nanofibers have been used as pyroelectric smart materials. Smart material based on Portland cement was tested to capture ambient thermal energy from pavements, which can be stored in capacitors for use as power sources to other sensor electronics. When carbon nanofibers were added, the cement-based composite was shown to act as a pyroelectric material. Addition of carbon nanofibers further increased the pyroelectric properties of the cement [86].

In order to improve the effectiveness of the energy conversion from heat to electricity, the 'Synchronized Switch Harvesting on Inductor' (SSHI) technique has been introduced [87] and was experimentally tested. SSHI was originally developed for energy harvesting from piezoelectric materials [87], and later expanded to pyroelectric energy harvesting [88]. The method proposed adding a switching device in parallel with the piezoelectric or pyroelectric materials. The switch and an inductance are in series. Opening and closing the switch is controlled to achieve enhanced energy harvesting from the material. The experimental study on pyroelectric materials found that for several amplitude variations of temperature from 0.5 to 8.0 K, the conversion efficiency is about 0.02% of the Carnot efficiency with a standard interface. Under the same heating conditions, experimental results showed that the SSHI technique increased the converted energy by a factor of about 2.5 times the standard interface, with which the efficiency was shown to practically become 0.05% of Carnot efficiency. The produced electrical power for a temperature amplitude of 7 K was more than 0.3 mW for an energy harvesting device composed of 8 g of active material [88].

5. Perspective, concluding remarks, and opportunities

With growing demand for energy harvesting from environmental sources for driving personal electronics and low-power devices, great excitement has been generated for using pyroelectric materials for converting heat to electricity. Although this conversion mechanism has been known for centuries, incorporation of nano- and microstructures into devices enabled by progress in nanomanufacturing and microfabrication technologies has provided a paradigm shift in energy harvesting. Since material properties often show size-dependent behavior, in particular in micro/nanoscale, there is need for quantitative characterization methods capable of measurement of small current/voltage generated from small-scale pyroelectrics. Currently there are no methods for measurement of pyroelectric effect in single-nanowire or single-microfiber level. Scanning probe microscopy methods may be applicable to these characterizations, which present a great opportunity of these techniques to enter pyroelectric energy harvesting field.

In addition, it is critical to intrinsically enhance the pyroelectric properties of the current materials using doping and material engineering. For example, *n*-doped or *p*-doped materials may exhibit different pyroelectric energy conversion. This is a great area of near term opportunity. For example, effect of doping and synthesis of nanowires could be quantified through development of rigorous experimental methods capable of identifying changes in the harvested energy from single nanowires. There are great opportunities for incorporation of pyroelectric materials, in particular nanowires and nanofibers, into flexible textile and wearable electronics for hybrid pyroelectric and

piezoelectric energy harvesting. These energy harvesters could power personal electronics and replace batteries.

Although, micro/nanoscale energy harvesting based on pyroelectric materials is a rather new field, it has already shown great promise and it is expected that the exciting near-term results will further stimulate research and development in this field.

References

[1] S. Chalasani and J.M. Conrad, *A Survey of Energy Harvesting Sources for Embedded Systems*, IEEE Southeastcon, Huntsville, AL, 2008, pp. 442–447.

[2] S.P. Beeby, M.J. Tudor, and N.M. White, *Energy harvesting vibration sources for microsystems applications*, Meas. Sci. Technol. 17 (2006), p. R175.

[3] A. Khaligh, P. Zeng, and C. Zheng, *Kinetic energy harvesting using piezoelectric and electromagnetic technologies – state of the art*, IEEE Trans. Indus. Electron. 57 (2010), pp. 850–860.

[4] S. Roundy, E.S. Leland, J. Baker, E. Carleton, E. Reilly, E. Lai, B. Otis, J.M. Rabaey, P.K. Wright, and V. Sundararajan, *Improving power output for vibration-based energy scavengers*. IEEE Pervasive Comput. 4 (2005), pp. 28–36.

[5] C. Lu, V. Raghunathan, and K. Roy, *Micro-scale energy harvesting: A system design perspective*, 15th Asia and South Pacific Design Automation Conference (Asp-Dac 2010), Taipei, IEEE Press, Piscataway, NJ, 2010, pp. 87–92.

[6] H.-B. Fang, J.-Q. Liu, Z.-Y. Xu, L. Dong, L. Wang, D. Chen, B.-C. Cai, and Y. Liu, *Fabrication and performance of MEMS-based piezoelectric power generator for vibration energy harvesting*, Microelectron. J. 37 (2006), pp. 1280–1284.

[7] D. Qian, W.K. Liu, and Q.J. Zheng, *Concurrent quantum/continuum coupling analysis of nanostructures*, Comp. Methods Appl. Mech. Eng. 197 (2008), pp. 3291–3323.

[8] J.P. Carmo, L.M. Gonçalves, and J.H. Correia, *Thermoelectric microconverter for energy harvesting systems*, IEEE Trans. Indus. Electron. 57 (2010), pp. 861–867.

[9] P. Markowski, W. Pinczakowski, L. Straszewski, and A. Dziedzic, *Thick-Film Thermoelectric Microgenerators Based on Nickel-, Silver-and PdAg-Based Compositions,* 30th International Spring Seminar on Electronics Technology, Cluj-Napoca, May 2007, pp. 223–228.

[10] W. Wang, F. Jia, Q. Huang, and J. Zhang, *A new type of low power thermoelectric microgenerator fabricated by nanowire array thermoelectric material*, Microelectron. Eng. 77 (2005), pp. 223–229.

[11] M. Grätzel, *Solar energy conversion by dye-sensitized photovoltaic cells*, Inorganic Chem. 44 (2005), pp. 6841–6851.

[12] W.-Y. Wong and C.-L. Ho, *Organometallic photovoltaics: A new and versatile approach for harvesting solar energy using conjugated polymetallaynes*, Accounts Chem. Res. 43 (2010), pp. 1246–1256.

[13] S.P. Beeby, R. Torah, M. Tudor, P. Glynne-Jones, T. O'Donnell, C. Saha, and S. Roy, *A micro electromagnetic generator for vibration energy harvesting*, J. Micromech. Microeng. 17 (2007), p. 1257.

[14] P. Glynne-Jones, M. Tudor, S. Beeby, and N. White, *An electromagnetic, vibration-powered generator for intelligent sensor systems*, Sens. Actuators A: Phys. 110 (2004), pp. 344–349.

[15] I. Sari, T. Balkan, and H. Kulah, *An electromagnetic micro power generator for wideband environmental vibrations*, Sens. Actuators A: Phys. 145 (2008), pp. 405–413.

[16] G. Sebald, D. Guyomar, and A. Agbossou, *On thermoelectric and pyroelectric energy harvesting*, Smart Mater. Struct. 18 (2009), p. 125006.

[17] S.K.T. Ravindran, T. Huesgen, M. Kroener, and P. Woias, *A self-sustaining micro thermomechanic-pyroelectric generator*, Appl. Phys. Lett. 99 (2011), p. 104102.

[18] J. Fang, H. Frederich, and L. Pilon, *Harvesting nanoscale thermal radiation using pyroelectric materials*, J. Heat Transfer 132 (2010), p. 092701.

[19] A. Navid, D. Vanderpool, A. Bah, and L. Pilon, *Towards optimization of a pyroelectric energy converter for harvesting waste heat*, Int. J. Heat Mass Transfer 53 (2010), pp. 4060–4070.

[20] G. Sebald, E. Lefeuvre, and D. Guyomar, *Pyroelectric energy conversion: Optimization principles*, IEEE Trans. Ultrasonics Ferroelectrics Freq. Control 55 (2008), pp. 538–551.
[21] R.C. Moreno, B.A. James, A. Navid, and L. Pilon, *Pyroelectric energy converter for harvesting waste heat: Simulations versus experiments*, Int. J. Heat Mass Transfer 55 (2012), pp. 4301–4311.
[22] D. Vanderpool, J.H. Yoon, and L. Pilon, *Simulations of a prototypical device using pyroelectric materials for harvesting waste heat*, Int. J. Heat Mass Transfer 51 (2008), pp. 5052–5062.
[23] R. Whatmore, *Pyroelectric devices and materials*, Reports Progress Phys. 49 (1986), p. 1335.
[24] S.B. Lang, *Pyroelectricity: From ancient curiosity to modern imaging tool*, Phys. Today 58 (2005), pp. 31–36.
[25] D. Vasileska and S.M. Goodnick, *Nano-Electronic Devices*, Springer, Berlin, 2011.
[26] R.W. Munn, *Theory of piezoelectricity, electrostriction, and pyroelectricity in molecular crystals*, J. Chem. Phys. 132 (2010), p. 104512.
[27] M. Srinivasan, *Pyroelectric materials*, Bull. Mater. Sci. 6 (1984), pp. 317–325.
[28] C.-P. Ye, T. Tamagawa, and D.L. Polla, *Experimental studies on primary and secondary pyroelectric effects in Pb(Zr[sub x]Ti[sub 1 - x])O[sub 3], PbTiO[sub 3], and ZnO thin films*, J. Appl. Phys. 70 (1991), pp. 5538–5543.
[29] S. Stokowski, *Thermal modulation transfer function analysis of pyroelectric device characteristics*, Appl. Optics 15 (1976), pp. 1767–1774.
[30] I. Lubomirsky and O. Stafsudd, *Invited review article: Practical guide for pyroelectric measurements*, Rev. Sci. Instrum. 83 (2012), p. 051101.
[31] A.N. Morozovska, E.A. Eliseev, G.S. Svechnikov, and S.V. Kalinin, *Pyroelectric response of ferroelectric nanowires: Size effect and electric energy harvesting*, J. Appl. Phys. 108 (2010), p. 042009-6.
[32] A. Hossain and M.H. Rashid, *Pyroelectric detectors and their applications*, IEEE Trans. Indus. Appl. 27 (1991), pp. 824–829.
[33] R.E. Newnham, *Properties of Materials: Anisotropy, Symmetry, Structure,* Oxford University Press, Oxford, 2005.
[34] A.H. Sahraoui, S. Longuemart, D. Dadarlat, S. Delenclos, C. Kolinsky, and J. Buisine, *Analysis of the photopyroelectric signal for investigating thermal parameters of pyroelectric materials*, Rev. Sci. Instrum. 74 (2003), pp. 618–620.
[35] T.P. Russell and J. Lutkenhaus, Nanotubes, nanorods and nanowires having piezoelectric and/or pyroelectric properties and devices manufactured therefrom, ed: US 8179026 B2, 2012.
[36] J. Wooldridge, J.F. Blackburn, N.L. McCartney, M. Stewart, P. Weaver, and M.G. Cain, *Small-scale piezoelectric devices: Pyroelectric contributions to the piezoelectric response*, J. Appl. Phys. 107 (2010), pp. 104118–104118-6.
[37] J.A. Geuther and Y. Danon, *High-energy x-ray production with pyroelectric crystals*, J. Appl. Phys. 97 (2005), pp. 104916–104916-5.
[38] A. Bykhovski, V. Kaminski, M. Shur, Q. Chen, and M. Khan, *Pyroelectricity in gallium nitride thin films*, Appl. Phys. Lett. 69 (1996), pp. 3254–3256.
[39] M. Shur, Pyroelectric and piezoelectric properties of gan-based materials, in *GaN and Related Alloys: Symposium Held November 29-December 4, 1998, Boston, Massachusetts, USA*, M.S. Shur, A.D. Bykhovski, and R. Gaska, eds., Material Research Society, Warrendale, PA, 1999.
[40] H. Yu, B. Kang, C. Park, U. Pi, C. Lee, and S.-Y. Choi, *The fabrication technique and electrical properties of a free-standing GaN nanowire*, Appl. Phys. A 81 (2005), pp. 245–247.
[41] C. Jagadish and S.J. Pearton, *Zinc Oxide Bulk, Thin Films and Nanostructures: Processing, Properties, and Applications*, Elsevier, Amsterdam, 2011.
[42] S. Lee, *ZnO and GaN nanostructures and their applications*, in *Oxide and Nitride Semiconductors*, T. Yao and S.-K. Hong, eds., Springer, Berlin, 2009, pp. 459–505.
[43] Y. Yang, W. Guo, K.C. Pradel, G. Zhu, Y. Zhou, Y. Zhang, Y. Hu, L. Lin, and Z.L. Wang, Pyroelectric nanogenerators for harvesting thermoelectric energy, *Nano Lett*. 12 (2012), pp. 2833–2838.
[44] I. Lubomirsky and O. Stafsudd, *Invited review article: Practical guide for pyroelectric measurements*, Rev. Sci. Instrum. 83 (2012), p. 051101-18.
[45] R.L. Byer and C. Roundy, *Pyroelectric coefficient direct measurement technique and application to a NSEC response time detector*, Ferroelectrics 3 (1972), pp. 333–338.

[46] B. Bhatia, J. Karthik, T. Tong, D.G. Cahill, L. Martin, and W. King, *Pyroelectric current measurements on PbZr0. 2Ti0. 8O3 epitaxial layers*, J. Appl. Phys. 112 (2012), p. 104106.
[47] A.M.D. Guzzi Plepis, G. Goissis, and D.K. Das-Gupta, *Dielectric and pyroelectric characterization of anionic and native collagen*, Polymer Eng. Sci. 36 (1996), pp. 2932–2938.
[48] S.B. Lang and D. Das-Gupta, *Laser intensity modulation method: A technique for determination of spatial distributions of polarization and space charge in polymer electrets*, J. Appl. Phys. 59 (1986), pp. 2151–2160.
[49] N. Shtykov and J. Vij, *Measurement of the polarization profile across a surface-stabilized ferroelectric liquid crystal cell using the pyroelectric laser-intensity-modulation method*, J. Appl. Phys. 93 (2003), pp. 159–164.
[50] S. Lang, *An analysis of the integral equation of the surface laser intensity modulation method using the constrained regularization method*, IEEE Trans. Dielectrics Electr. Insulation 5 (1998), pp. 70–76.
[51] S. Domanski, *The dependence of the coercive field of tri-glycine sulphate on temperature and frequency*, Proc. Phys. Soc. 72 (1958), p. 306.
[52] S.B. Lang and F. Steckel, *Method for the measurement of the pyroelectric coefficient, dc dielectric constant, and volume resistivity of a polar material*, Rev. Sci. Instrum. 36 (1965), pp. 929–932.
[53] A. Glass, *Investigation of the electrical properties of* $Sr_{1-x}Ba_xNb_2O_6$ *with special reference to pyroelectric detection*, J. Appl. Phys. 40 (1969), pp. 4699–4713.
[54] R.W. Whatmore, *Pyroelectric devices and materials*, Rep. Prog. Phys. 49 (1986), pp. 1335–1386.
[55] G.C. Mavropoulos, *Unsteady heat conduction phenomena in internal combustion engine chamber and exhaust manifold surfaces*, in *Heat Transfer – Engineering Applications*, V. Vikhrenko, InTech, 2011, DOI: 10.5772/26369, ISBN: 978-953-307-361-3. Available at http://www.intechopen.com/books/heat-transfer-engineering-applications/unsteady-heat-conduction-phenomena-in-internal-combustion-engine-chamber-and-exhaust-manifold-surfac
[56] G. Cha and Y.S. Ju, *Pyroelectric energy harvesting using liquid-based switchable thermal interfaces*, Sens. Actuators A-Phys. 189 (2013), pp. 100–107.
[57] P. Mane, J.S. Xie, K.K. Leang, and K. Mossi, *Cyclic energy harvesting from pyroelectric materials*, IEEE Trans. Ultrasonics Ferroelectrics Freq. Control 58 (2011), pp. 10–17.
[58] H.H.S. Chang and Z. Huang, *Laminate composites with enhanced pyroelectric effects for energy harvesting*, Smart Mater. Struct. 19 (2010), p. 065018.
[59] X.-C. Zheng, G.-P. Zheng, Z. Lin, and Z.-Y. Jiang, *Thermo-electrical energy conversions in Bi0.5Na0.5TiO3–BaTiO3 thin films prepared by sol–gel method*, Thin Solid Films 522 (2012), pp. 125–128.
[60] K. Huang, J.B. Wang, X.L. Zhong, B.L. Liu, T. Chen, and Y.C. Zhou, *Significant polarization variation near room temperature of Ba0.65Sr0.35TiO3 thin films for pyroelectric energy harvesting*, Sens. Actuators B: Chem. 169 (2012), pp. 208–212.
[61] A. Cuadras, M. Gasulla, and V. Ferrari, *Thermal energy harvesting through pyroelectricity*, Sens. Actuators A-Phys. 158 (2010), pp. 132–139.
[62] R.A. Bernal, R. Agrawal, B. Peng, K.A. Bertness, N.A. Sanford, A.V. Davydov, and H.D. Espinosa, *Effect of growth orientation and diameter on the elasticity of GaN nanowires: A combined in situ TEM and atomistic modeling investigation*, Nano Lett. 11 (2010), pp. 548–555.
[63] Y. Yang, J.H. Jung, B.K. Yun, F. Zhang, K.C. Pradel, W. Guo, and Z.L. Wang, *Flexible pyroelectric nanogenerators using a composite structure of lead-free* $KNbO_3$ *Nanowires*, Adv. Mater. 24 (2012), pp. 5357–5362.
[64] Z.L. Wang, *Splendid one-dimensional nanostructures of zinc oxide: A new nanomaterial family for nanotechnology*, ACS Nano. 2 (2008), pp. 1987–1992.
[65] M. Minary-Jolandan, R.A. Bernal, I. Kujanishvili, V. Parpoil, and H.D. Espinosa, *Individual GaN nanowires exhibit strong piezoelectricity in 3D*, Nano Lett. 12 (2012), pp. 970–976.
[66] M. Minary-Jolandan, R.A. Bernal, and H.D. Espinosa, *Strong piezoelectricity in individual GaN nanowires*, MRS Commun. 1 (2011), pp. 45–48.
[67] H.D. Espinosa, R.A. Bernal, and M. Minary-Jolandan, *A review of mechanical and electromechanical properties of piezoelectric nanowires*, Adv. Mater. 24 (2012), pp. 4656–4675.

[68] A.I. Boukai, Y. Bunimovich, J. Tahir-Kheli, J.-K. Yu, W.A. Goddard III, and J.R. Heath, *Silicon nanowires as efficient thermoelectric materials*, Nature 451 (2008), pp. 168–171.
[69] A.I. Hochbaum, R. Chen, R.D. Delgado, W. Liang, E.C. Garnett, M. Najarian, A. Majumdar, and P. Yang, *Enhanced thermoelectric performance of rough silicon nanowires*, Nature 451 (2008), pp. 163–167.
[70] Y. Yang, Y. Zhou, J.M. Wu, and Z.L. Wang, *Single micro/nanowire pyroelectric nanogenerators as self-powered temperature sensors*, ACS Nano. 6 (2012), pp. 8456–8461.
[71] Y. Yang, H.L. Zhang, G. Zhu, S. Lee, Z.H. Lin, and Z.L. Wang, *Flexible hybrid energy cell for simultaneously harvesting thermal, mechanical, and solar energies*, ACS Nano 7 (2013), pp. 785–790.
[72] N. Chocat, G. Lestoquoy, Z. Wang, D.M. Rodgers, J.D. Joannopoulos, and Y. Fink, *Piezoelectric fibers for conformal acoustics*, Adv. Mater. 24 (2012), pp. 5327–5332.
[73] L. Persano, C. Dagdeviren, Y. Su, Y. Zhang, S. Girardo, D. Pisignano, Y. Huang, and J.A. Rogers, *High performance piezoelectric devices based on aligned arrays of nanofibers of poly (vinylidenefluoride-co-trifluoroethylene)*, Nat. Commun. 4 (2013), p. 1633.
[74] M. Lee, C.Y. Chen, S. Wang, S.N. Cha, Y.J. Park, J.M. Kim, L.J. Chou, and Z.L. Wang, *A hybrid piezoelectric structure for wearable nanogenerators (vol. 24, pp. 1759, 2012)*, Adv. Mater. 24 (2012), pp. 5283–5283.
[75] T. Subbiah, G.S. Bhat, R.W. Tock, S. Parameswaran, and S.S. Ramkumar, *Electrospinning of nanofibers*, J. Appl. Polymer Sci. 96 (2005), pp. 557–569.
[76] F.A. He, M. Sarkar, S. Lau, J.T. Fan, and L.H. Chan, *Preparation and characterization of porous poly(vinylidene fluoride-trifluoroethylene) copolymer membranes via electrospinning and further hot pressing*, Polymer Testing 30 (2011), pp. 436–441.
[77] M. Lee, C.Y. Chen, S. Wang, S.N. Cha, Y.J. Park, J.M. Kim, L.J. Chou, and Z.L. Wang, A *hybrid piezoelectric structure for wearable nanogenerators*, Adv. Mater. 24 (2012), pp. 1759–1764.
[78] H. Nguyen, A. Navid, and L. Pilon, *Pyroelectric energy converter using co-polymer P(VDF-TrFE) and Olsen cycle for waste heat energy harvesting*, Appl. Thermal Eng. 30 (2010), pp. 2127–2137.
[79] C.P.J. Kulek, and E. Markiewicz, *Influence of poling and ageing on high frequency dielectric and piezoelectric response of PVDF-type polymer foils*, J. Electrost. 56 (2002), pp. 135–141.
[80] T. Mirfakhrai, J.D.W. Madden, and R.H. Baughman, *Polymer artificial muscles,* Mater. Today 10 (2007), pp. 30–38.
[81] V. Sencadas, R. Gregorio, and S. Lanceros-Méndez, *α to β phase transformation and microestructural changes of PVDF films induced by uniaxial stretch*, J. Macromol. Sci. Part B. 48 (2009), pp. 514–525.
[82] R. Kandilian, A. Navid, and L. Pilon, *The pyroelectric energy harvesting capabilities of PMN–PT near the morphotropic phase boundary*, Smart Mater. Struct. 20 (2011), p. 055020.
[83] I.M. McKinley and L. Pilon, *Phase transitions and thermal expansion in pyroelectric energy conversion*, Appl. Phys. Lett. 102 (2013), p. 023906.
[84] F.Y. Lee, A. Navid, and L. Pilon, *Pyroelectric waste heat energy harvesting using heat conduction*, Appl. Thermal Eng. 37 (2012), pp. 30–37.
[85] F.Y. Lee, S. Goljahi, I.M. McKinley, C.S. Lynch, and L. Pilon, *Pyroelectric waste heat energy harvesting using relaxor ferroelectric 8/65/35 PLZT and the Olsen cycle*, Smart Mater. Struct. 21 (2012), p. 025021.
[86] S. Bhattacharjee, A. Batra, S. Meseret, and J. Cain, *High-performance single and polycrystal-based pyroelectric smart materials for energy harvesting from pavements*, Transport. Res. Record: J. Transport. Res. Board 2252 (2011), pp. 75–82.
[87] D. Guyomar, A. Badel, E. Lefeuvre, and C. Richard, *Toward energy harvesting using active materials and conversion improvement by nonlinear processing*, IEEE Trans. Ultrasonics Ferroelectrics Freq. Control 52 (2005), pp. 584–595.
[88] D. Guyomar, G. Sebald, E. Lefeuvre, and A. Khodayari, *Toward heat energy harvesting using pyroelectric material*, J. Intell. Mater. Syst. Struct. 20 (2009), pp. 265–271.